Molecular Crystals and Liquid Crystals

Publication details, including instructions for authors and subscription information:
http://www.tandfonline.com/loi/gmcl20

Molecular Engineering the Phototransport Properties of Discotic Liquid Crystals

K. J. Donovan [a], T. Kreouzis [a], K. Scott [a], J. C. Bunning [a], R. J. Bushby [b], N. Boden [b], O. R. Lozman [b] & B. Movaghar [b]

[a] Physics Department, Queen Mary University of London, MileEnd Road, London, E1 4NS, UK

[b] SOMS Centre, University of Leeds, Leeds, LS2 9JT, UK

Version of record first published: 18 Oct 2010

To cite this article: K. J. Donovan, T. Kreouzis, K. Scott, J. C. Bunning, R. J. Bushby, N. Boden, O. R. Lozman & B. Movaghar (2003): Molecular Engineering the Phototransport Properties of Discotic Liquid Crystals, Molecular Crystals and Liquid Crystals, 396:1, 91-112

To link to this article: http://dx.doi.org/10.1080/15421400390213221

Mol. Cryst. Liq. Cryst., Vol. 396, pp. 91–112, 2003

ISSN: 1542-1406 print/1563-5287 online
DOI: 10.1080/15421400390213221

Taylor & Francis
Taylor & Francis Group

MOLECULAR ENGINEERING THE PHOTOTRANSPORT PROPERTIES OF DISCOTIC LIQUID CRYSTALS

K. J. Donovan, T. Kreouzis, K. Scott, and J. C. Bunning*
Physics Department, Queen Mary University of London, Mile End Road, London E1 4NS, UK

R. J. Bushby, N. Boden, O. R. Lozman, and B. Movaghar
SOMS Centre, University of Leeds, Leeds, LS2 9JT, UK

This paper explores how charge carrier mobilities in columnar discotic liquid crystals may be enhanced. The hole mobility and its temperature dependence has been measured in a variety of triphenylene based DLC's using the time of flight method in the mesophase and where possible in the glassy (or crystalline) phase. A model using the Holstein small polaron is fitted to the results and the resulting polaron self energy and bandwidth are found. Where trapping is observed it shows a tendency to trap at a faster rate as electric field is increased. This is discussed in terms of dimensionality of the carrier transport. Some transient data is fitted to the Noolandi multiple trapping model and trapping rates and detrapping rates using that model are recovered. Their variation with electric field is discussed.

Keywords: photoconductivity–thin films, 73.50.P; Polarons, 71.38; time of flight; transport processes–thin films, 73.50, 73.61; molecular electronic devices, 85.65

I. INTRODUCTION

From their structure it has been anticipated that discotic liquid crystals would display interesting charge transport properties. Because of this they have been the object of many studies into their phototransport properties [1–4]. The expectation arises because the discotics form columnar structures with conjugated macrocycles stacking face to face with their neighbours offering the possibility of a large delocalisation (band motion) or high

We would like to thank the Leverhulme trust for supporting the time of flight measurements, Grant reference F/476/AB.

*Corresponding author. E-mail: k.j.Donovan@qmul.ac.uk

hopping/tunnelling rate between neighbouring molecules along a stack. The stacks are themselves arranged on a crystalline lattice with a hydrophobic, low electron affinity aliphatic region separating the adjacent stacks. Such aliphatic "waxy" regions are expected to offer a high degree of insulation between stacks and this leads to interesting questions concerning the role of dimensionality in the transport of charge along the stacks. Furthermore the molecules are self organising and their introduction into a cell of restricted thickness in one dimension will often result in the homeotropic alignment of the stacks along that dimension. This work describes the mobility of carriers along the stack direction as electric field and temperature is varied. The mobilities found are high for organic materials and molecular engineering is shown here to make a substantial improvement in mobility on the stacks. The materials reported here are based around the triphenylene motif and include the most widely studied of such materials, 2,3,6,7,10,11-Hexakis(hexyloxy)-triphenylene, **HAT6**. The mobility of this material along with **HAT11** has been reported previously [1,2]. The aliphatic chain length may be varied and we present results for **HAT3**, shown in Figure 1. The effect of the alkyl chain length on the mobility is explored. Among the smaller discogens studied, results are also presented for 1,4-Difluoro-2,3,6,7,10,11-Hexakis(hexyloxy)-triphenylene,

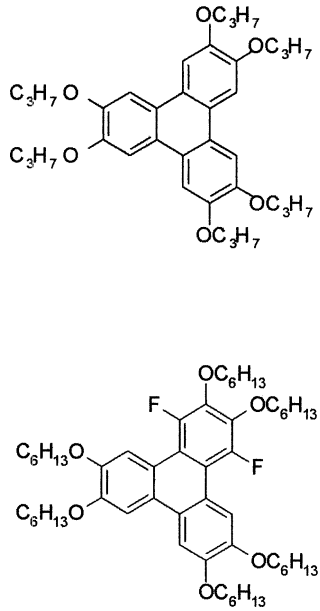

FIGURE 1 The molecules **HAT6** and **2FHAT6**, upper and lower structures respectively.

2FHAT6 also shown in Figure 1. Addition of larger discogens, shown in Figure 2, based on the triphenylenes, such as 2,3,6,7,10,11-Hexakis-(4-n-nonylphenyl)-triphenylene, **PTP9** 2,3,6,7,10,11-Hexakis-(4-n-hexyloxyphenyl)-triphenylene, **PTPO11** and 2,3,6,7,10,11-Hexakis(4-nonylphenyl)dipyrazino[2,3-f:2′,3′-h]-quinoxaline., **PDQ9**, with the smaller discogens **HAT6**, **HAT11** and **2FHAT6** in 50 : 50 stoichiometric mixtures are shown to increase the mobility substantially.

II. EXPERIMENTAL

In the experiments described here and in more detail in previous work [1,2,3], a thin cell is made up by taking two quartz slides, evaporating aluminium electrodes on one surface of each to form electrodes and holding the two surfaces in a cross configuration with the electrode surfaces parallel and separated by a dielectric spacer of controlled thickness, typically between 5 μm and 25 μm, in a rig in which the temperature can be varied. The stacks align parallel to the electrode surfaces and it is possible to apply electric fields along the stack direction in this way. It is now possible to carry out time of flight, TOF, measurements on samples with this geometry. One of the electrodes is made semitransparent and a 337 nm, 6 ns laser pulse from a nitrogen laser incident on this electrode is used to excite carriers in a thin absorption skin depth, $\delta \approx 0.1\,\mu m$, at the top of the stacks close to the electrode. An applied voltage, V, separates the electrons and holes in the applied electric field, $E = -V/d$. When the counter electrode is negative wrt the illuminated electrode, holes move down the stacks towards the counter electrode. This induces a transient photocurrent, $I(t)$, where the $I(t)$ transient changes from an initially almost time independent current plateau to a decaying $I(t)$ at some later time. This form of $I(t)$ may be used to infer, from the appearance of the kink, a TOF transit time, T_{Tr}. With knowledge of sample thickness, d, the velocity of holes

$$v = \frac{d}{T_{Tr}} \tag{1}$$

is found as the electric field is varied and thus their mobility, μ,

$$\mu = \frac{v}{E} = \frac{d^2}{VT_{Tr}} \tag{2}$$

may be inferred from the slope of a graph of v verses E. The variation of the mobility may then be found as the temperature is varied.

In all the results reported here only hole transits are found and the velocity of the holes are always found to be proportional to E.

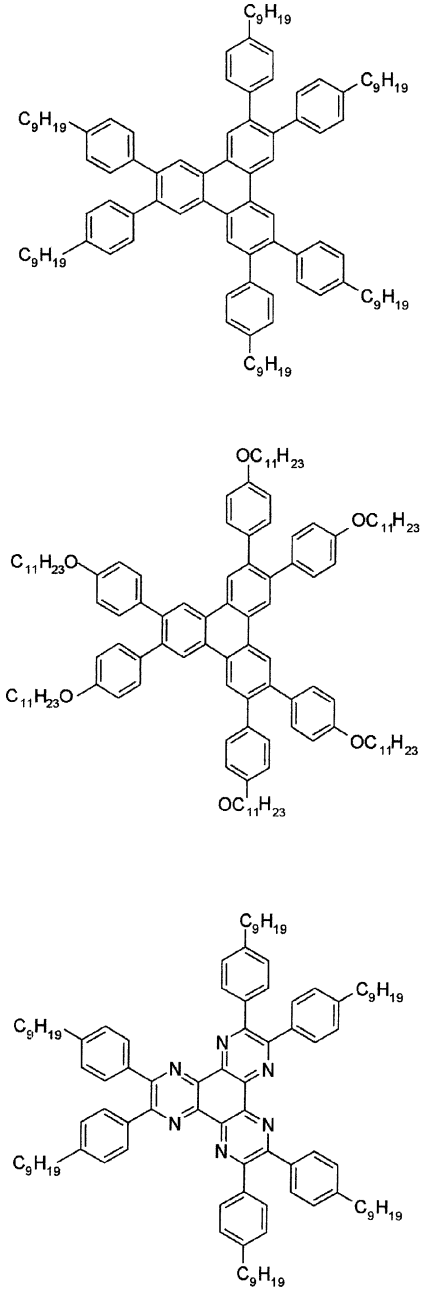

FIGURE 2 The molecules, **PTP9**, **PTPO11** and **PDQ9** from top to bottom.

III. RESULTS

IIIa. Results for Single Triphenylene Systems

Figures 3a, and 3b show transits measured in the discotic phase of these materials for **HAT3** and **2FHAT6** respectively. Transits for **HAT6** and **HAT11**in the mesophase have been shown previously [2]. **HAT6** and **HAT11** show no TOF transit signals in their crystalline phase where the carriers are found to trap in a distance less than the sample thickness with a featureless decay being typical of the trapping. The new materials reported here, **HAT3** and **2FHAT6,** show TOF transit behaviour throughout the temperature range until the isotropic phase is reached.

Finding v from such data and plotting v verses E the mobility was found for these materials and its variation with temperature is shown in Figures 4a and 4b for **HAT3** and **2FHAT6** respectively. The temperature dependence for the hole mobility in **HAT6** and **HAT11** have been shown previously [5].

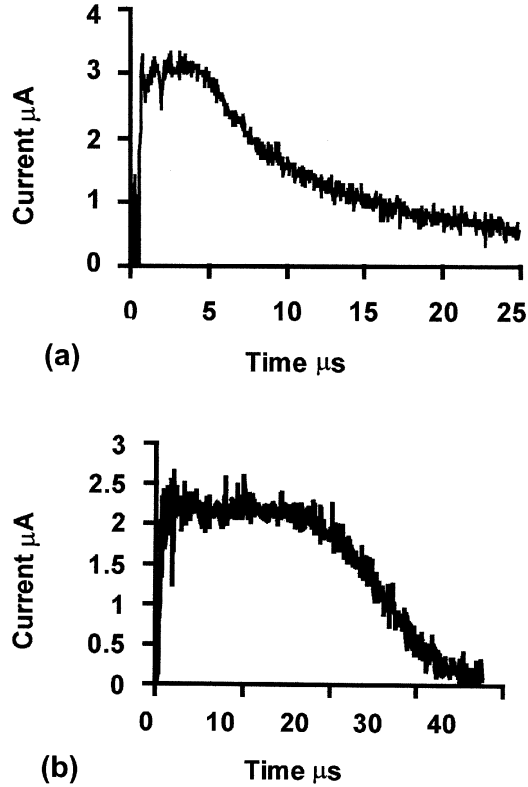

FIGURE 3 Photocurrent transits in the mesophase of a) **HAT3** and b) **2FHAT**.

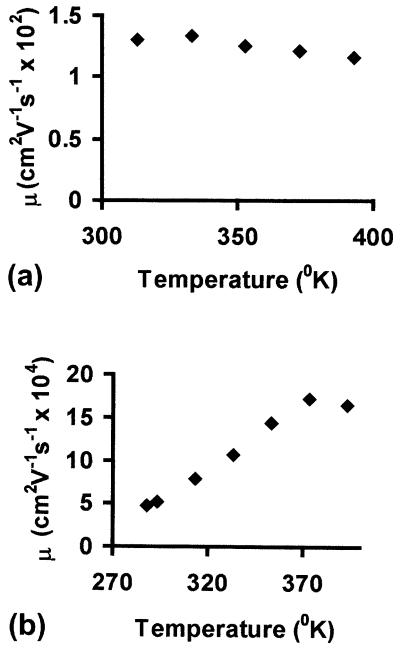

FIGURE 4 a) Variation of hole mobility with temperature for **HAT3** and b) for **2FHAT6**.

IIIb. Results for Binary Discotic Systems

Figures 5a, 5b and 5c show transit signals in the discotic mesophase for **2FHAT6 : PTP9**, **HAT6 : PDQ9** and **HAT6 : PTPO11** respectively. Transit signals for the binary systems **HAT6 : PTP9** and **HAT11 : PTP9** have also been shown previously [2]. Such transit signals are again found throughout the temperature range until the isotropic phase is reached. This is also true of the two binaries previously reported. Once again μ is found for these materials and Figures 6a, 6b and 6c show the variation of μ with temperature for **2FHAT6 : PTP9, HAT6 : PDQ9** and **HAT6 : PTPO11** respectively. The variations of μ with temperature for **HAT6 : PTP9**, **HAT11 : PTP9** have been previously presented [5].

IV. DISCUSSION

IVa. Hole Mobilities in Single Molecule Systems vs Binary Systems

We have measured the hole mobilities in nine materials. The immediately evident fact about the values of mobility found and gathered together in

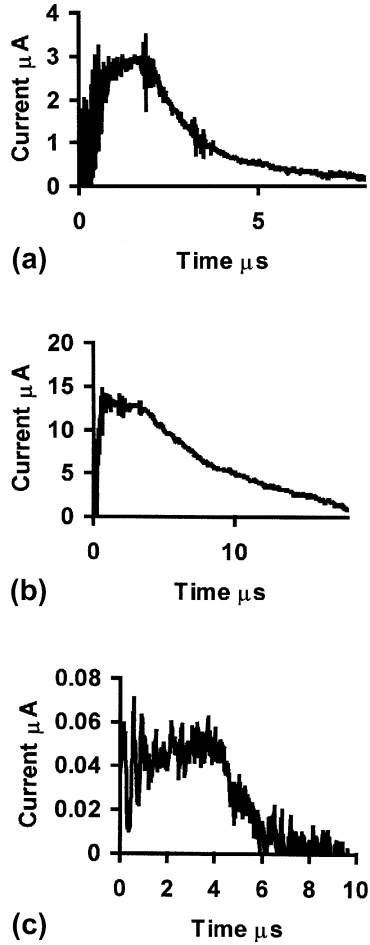

FIGURE 5 Photocurrent transits in the mesophase of a) **2FHAT6 : PTP9**, b) **HAT6 : PDQ9**, c) **HAT6 : PTPO11**.

Table 1 is that by mixing **HAT11**, **HAT6** or **2FHAT6** with any of the large discogens leads to a substantially enhanced mobility. In the case of **HAT11** and **HAT11 : PDP9** the change in mobility amounts to a factor of 260. This enhancement in mobility it is proposed is due to an increase in the ordering along the column for the binary mixtures compared with the smaller triphenylenes alone. This ordering comes about as a result of the way triphenylene molecules alternate with the larger discogens down the stack. Molecular modelling has shown such an arrangement leads to a reduction in interfacial energies [6] and is thus favoured. X-ray diffraction evidence also

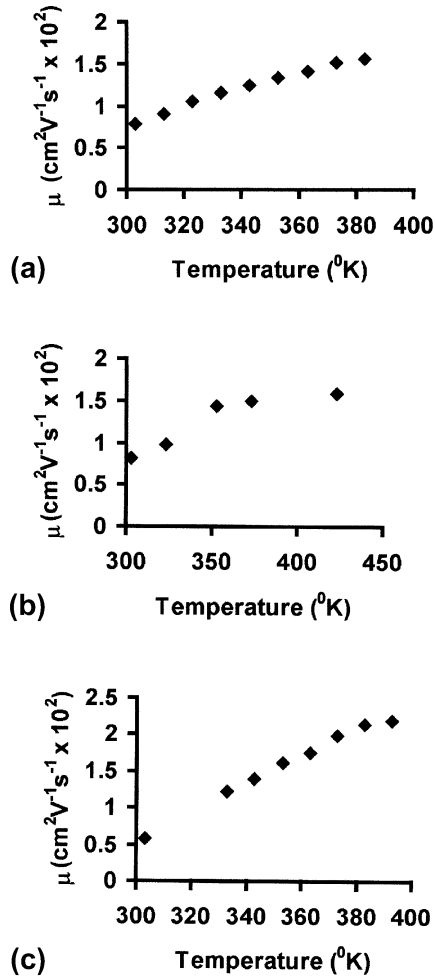

FIGURE 6 Variation of hole mobility with temperature for a) **2FHAT6 : PTP9**, b) **HAT6 : PDQ9** and c) **HAT6 : PTPO11**.

indicates greater ordering and in particular that there is an interleaving of the larger molecules on one stack with smaller molecules on neighbouring stacks [6] and it is this that may induce the greater three dimensional ordering. The fact that transits are observable in the glassy phase for the binaries also lends support to the existence of greater ordering and consequent increase in S, the distance a carrier may travel before deep trapping at some defect. It is of interest to note the large mobility found here for **HAT3**, where it is comparable to the mobilities found in the binary

TABLE 1 The Electronic Properties of Hole Carriers in the Discotic Systems Studied Here Including Hole Mobility, Polaron Binding Energy and Polaron Bandwidth

Material	Polaron Energy, E_P	Polaron Bandwidth, J (meV)	Hole Mobility, μ ($cm^2 V^{-1} s^{-1}$)
HAT6[a]	181 meV	3	7.8×10^{-4}
HAT11[a]	690 meV	165	1.10×10^{-4}
HAT6 : PTP9[a]	203 meV	23	2.3×10^{-2}
HAT11 : PTP9[a]	113 meV	10	2.9×10^{-2}
HAT3[b]	24 meV	10	1.3×10^{-2}
2FHAT6[b]	372 meV	30	1.6×10^{-3}
2FHAT6 : PTP9[b]	260 meV	32	1.5×10^{-2}
HAT6 : PDQ9[b]	224 meV	23	1.6×10^{-2}
HAT6 : PTPO11[b]	4.1 eV	50	2.0×10^{-2}

[a]T. Kreouzis et al, J. Chem. Phys., 114, 1797 2001.
[b]This work.

materials. This is in line with observations made by others on **HAT4** [7] where a mobility of $1.2 \times 10^{-2}\,cm^2\,V^{-1}\,s^{-1}$ has been reported. Figure 7 shows the hole mobility in the mesophase of the five **HATn** molecules so far studied as n is varied. We have included the results reported for **HAT5** [8] with a low value for the mobility of $8.0 \times 10^{-4}\,cm^2\,V^{-1}\,s^{-1}$. There is a marked discontinuity in the mobility as it increases rapidly on passing from the columnar hexagonal, Col_h, phase of **HAT5** to the columnar hexagonal plastic, Col_{hp}, phase of **HAT4**. This discontinuity is maintained either side of the **HAT5**/**HAT4** boundary. There is evidence of three dimensional ordering in the x-ray analysis of the **HAT3** and **HAT4** materials and they have been designated as plastic columnar phases. This is another example, along with

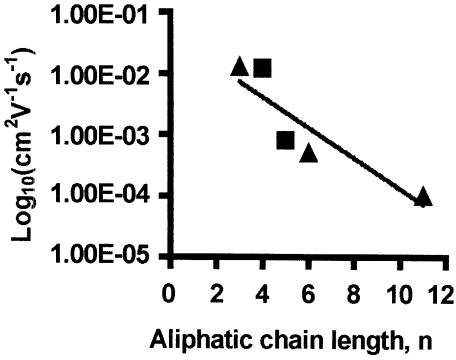

FIGURE 7 The change in hole mobility for **HATn** as n is changed. The data for n = 4 and 5, ■, are from [7] and [8] respectively.

the binaries, of the imposition of three dimensional ordering leading to substantial increases in the mobility.

IVb. Temperature Dependence and the Holstein Polaron

It has been previously noted that the hole mobility for **HAT6** and **HAT11** is surprisingly weakly dependent on temperature given the dynamic fluctuations occurring in the mesophase that would be expected to give rise to a strongly temperature dependent scattering. In particular there are the fluctuations in intermolecular spacing along the stacks characteristic of the liquid crystal state. There are also rotational modes of displacement of the discotic molecules about an axis along the stack direction. Both of these may be expected to cause significant scattering via their influence on the intermolecular overlap integral. Other authors [9] have sought to explain this weak temperature dependence by showing that the effects of the rotational fluctuations and the longitudinal fluctuations have opposite effects on the mobility as temperature is increased and within a small range of parameters these effects can be made to cancel each other out. When it became clear that there was a weakly temperature dependent mobility in the two binary mixtures, **HAT6 : PTP9** and **HAT11 : PTP9** even as the materials passed from the discotic mesophase into the glassy phase this mechanism became a little difficult to continue with. It was then suggested [5] that an alternative explanation may lie in the polaron first described by Holstein [10,11]. In the new results presented here we demonstrate materials that possess strongly temperature dependent hole mobilities such as **2FHAT6** in Figure 4b and **HAT6 : PTPO11** in Figure 6c as well as materials where the dependence is still weak such as **HAT3** in Figure 4a and **HAT6 : PDQ9** in Figure 6b.

Holsteins polaron theory was developed to describe the diffusivity of charge on a one dimensional array of diatomic atoms thus reducing the degrees of freedom necessary in describing the problem. With an electron present on the diatomic molecule the spring constant changes and the energy of the electron in the LUMO of that molecule is reduced by the polaron binding energy, E_P. For the electron to move between neighbouring molecules an interaction J between them is required also required are thermal fluctuations in the conformation of the neighbouring molecules to allow isoenergetic transitions.

The small polaron results when the lifetime of the carrier against scattering is shortened to the extent that the energy uncertainty associated with the lifetime is greater than the polaron bandwidth and the carrier wavefunction is then effectively localised. One result from this theory is that there exist two regimes to describe the carrier diffusivity. In Holsteins tour de force it can be hard to discover the required quantities for

comparison with experiment so we follow Pope and Swenberg [12] who have given a clarified account of these matters in their book.

In the adiabatic limit with a large J that is comparable to the polaron binding energy, the carrier moves from site to site overcoming a potential barrier between sites with a resulting activated mobility not unlike the conventional hopping description:

$$\mu = \frac{ea^2\omega_0}{k_BT}\exp\left(\frac{-\left(\frac{1}{2}E_P - J\right)}{k_BT}\right) \tag{3}$$

Here, a is the lattice spacing and $\omega_0$is an attempt rate or optic phonon frequency.

In the nonadiabatic limit with $J \ll E_P$ the mobility is:

$$\mu = \frac{ea^2}{kT}\frac{1}{\hbar}\left(\frac{\pi}{2E_Pk_BT}\right)^{\frac{1}{2}}J^2\exp\left(\frac{-E_P}{2k_BT}\right) \tag{4}$$

In both Eqs. (3) and (4) the temperature appears in a pre-exponential factor as well as in the exponential and this may cause the temperature dependence over a limited temperature range to appear very weak as is often the case in these results.

For molecular crystals with strong electron-phonon coupling and narrow bands it is the case that $E_P > J$ and we take the latter case. Plotting $\log_e(\mu T^{1.5})$ against T^{-1} the Holstein polarom would give a straight line with slope S given by:

$$S = \frac{-E_P}{2k_BT} \tag{5}$$

and intercept on the log axis, I given by:

$$I = \frac{ea^2}{k_B^{3/2}}\frac{1}{\hbar}\left(\frac{\pi}{2E_P}\right)^{1/2}J^2 \tag{6}$$

Such plots are shown in Figures 8 for the pure materials **HAT3** and **2FHAT6** and in Figures 9 for the binary mixtures **2FHAT6 : PTP9**, **HAT6 : PDQ** and **HAT6 : PTPO11**. All of these materials show an excellent fit to the predicted Holstein small polaron behaviour in the $J \ll E_P$ non-adiabatic limit. This is true whether there is a very weak dependence of μ on T such as for **HAT6** or a much faster variation as for **2FHAT6**. From these graphs values for E_P and J are recovered and Table 1 shows these values along with the values found previously for **HAT6**, **HAT11**, **HAT6 : PTP9** and **HAT11 : PTP9**. For all nine materials studied the analysis is self consistent in that $E_P > J$. **HAT6 : PTPO11** has, in this analysis

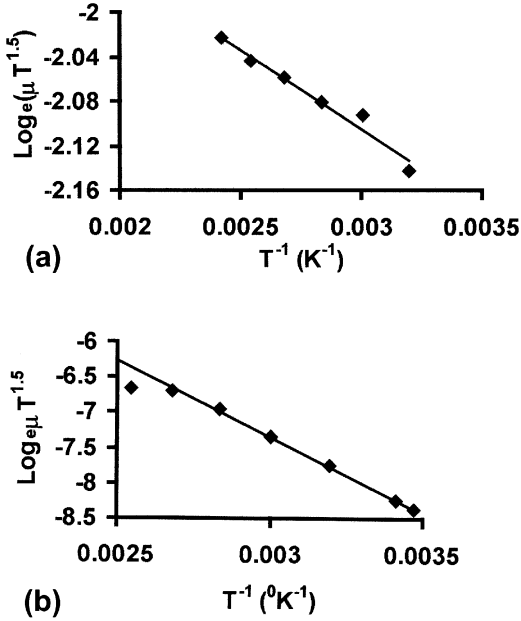

FIGURE 8 Plot of hole mobility vs Temperature according to Eq. (4) for a) **HAT3** and b) **2FHAT6**.

an unacceptably large polaron binding energy of 4.1 eV. The **HAT11** results also show large binding energy and bandwidth. In the case of this material however as was noted previously, the temperature range over which the mobility could be measured was severely limited with the mesophase having only 12°K range of existence between the crystalline and isotropic phases. With these exceptions the Holstein small polaron is able to explain the temperature dependence of the hole mobility over a wide range of materials. It is to be noted that an abrupt change in behaviour of the mobility at the discotic/crystalline (glassy) phase boundary is never observed notwithstanding the fact that for two materials, **HAT6** and **HAT11**, there is a severe reduction in carrier range on passing to the crystalline phase. The Holstein theory was developed to describe a homogenous linear chain of diatomic molecules with the interatomic separation being the single configuration co-ordinate playing the crucial role in perturbing the electron energy. In the case of the materials presented here we have no candidate for the configurational modes responsible for the behaviour. The discotic molecules themselves that form the chain will have a large number of configuration co-ordinates describing their vibrational behaviour. We note that in the present case the binaries

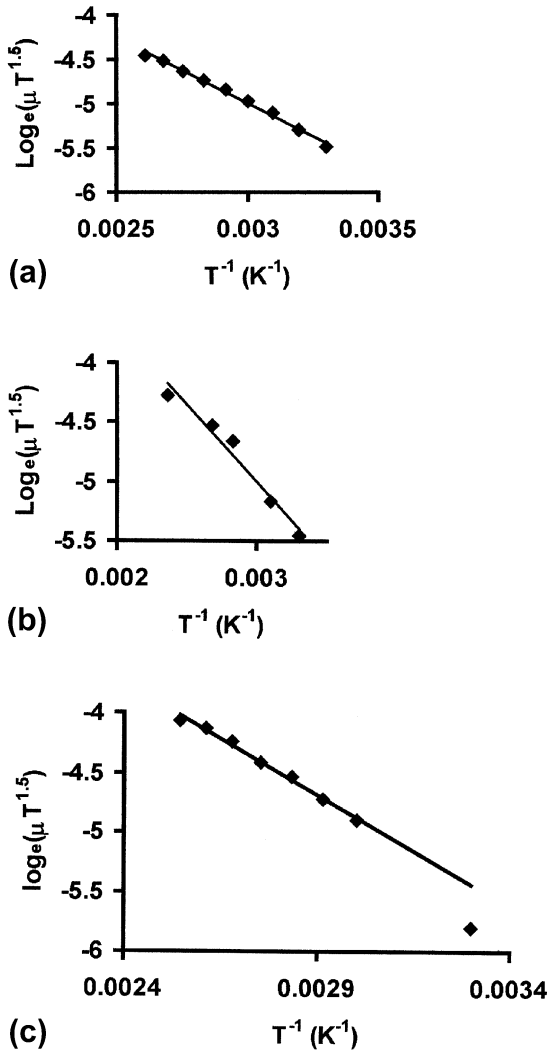

FIGURE 9 Plot of hole mobility vs Temperature according to Eq. (4) for a) **2FHAT6:PTP9**, b) **HAT6:PDQ9** and c) for **HAT6:PTPO11**.

have a chemical potential ΔG (currently unknown) between adjacent molecules that is absent from the Holstein model. The applied electric field also leads to a potential difference between adjacent sites although this amounts to no more than $k_BT/30$ at the largest fields used which is a small perturbation on the energies found here.

IVc. Trapping and Dimensionality

One of the interesting possibilities of the columnar materials is that they may display some reduced dimensionality effects in their charge transport properties as a result of the high wavefunction overlap along the column compared to that between columns separated by aliphatic insulators. To find such effects it has been necessary to look carefully at the trapping behaviour of the photocurrent in the crystalline phase of **HAT6** and at the tail on the transit in **HAT11 : PTP9**. In three dimensional, 3D, materials e.g. Silicon the trapping properties of the material is defined by the time, τ, taken to reach a trap which is a constant of the material independent of any external influence such as electric field. In one dimension, 1D, the important and invariant parameter for a carrier when describing trapping is the average separation between trapping sites, S. The time to trap in 1D will be inversely proportional to electric field. The carrier is taken to the trap by drift in the field in 1D whereas it is by diffusion in 3D. This difference is in effect a result of the number of new sites, N, visited by a carrier as it diffuses making n steps in 1D or 3D. It has been shown by Montroll and Weiss [13] that in 1D, N varies as $\sqrt{n}$ while in 3D N varies as n. This type of behaviour has been observed in for example the molecular charge transfer crystal, phenanthrene-pyromellitic acid dianhydride [14] by Haarer and Mohwald. In Figures 9a and 9b the transient photocurrent found in a **HAT6** sample at high and low field is shown. It is immediately clear that the current decays faster in the higher field as the carriers are brought to the trap site on the column at a faster rate through drift.

A very simple model [3] is sufficient to describe the shape of the current transients after an impulse of excess carriers due to a light pulse. This model takes a single set of traps, no trap depth distribution and an exponential trapping and detrapping rate with rate constants, ${\tau_1}^{-1}$ and ${\tau_2}^{-1}$ respectively.

The rate equations for the free and bound carriers, n_f and n_b are:

$$\frac{dn_f}{dt} = \frac{-n_f}{\tau_1} + \frac{n_b}{\tau_2} \tag{7}$$

$$\frac{dn_b}{dt} = \frac{-n_b}{\tau_2} + \frac{n_f}{\tau_1} \tag{8}$$

The boundary conditions are :

$$n_f(0) = n_0 \tag{9}$$

$$n_f(t) + n_b(t) = n_0 \tag{10}$$

The equations are easily solved to give an expression for the number of free carriers as follows:

$$n_f(t) = n_0\left[\frac{\tau_2}{\tau_1+\tau_2}\exp\left(\frac{-t}{\tau_{\text{eff}}}\right)+\frac{\tau_1}{\tau_1+\tau_2}\right] \tag{11}$$

The current is then

$$I(t) = I_0\left[\frac{\tau_2}{\tau_1+\tau_2}\exp\left(\frac{-t}{\tau_{\text{eff}}}\right)+\frac{\tau_1}{\tau_1+\tau_2}\right] \tag{12}$$

The solid lines on the data of Figures 10a and 10b are a fit of $I(t)$ to Eq. (12). They are found to fit the data very well for such a simple model. More sophisticated attempts to fit this data using stretched exponentials do not manage to provide a fit and including diffusion in the process gives considerably worse fits [1].

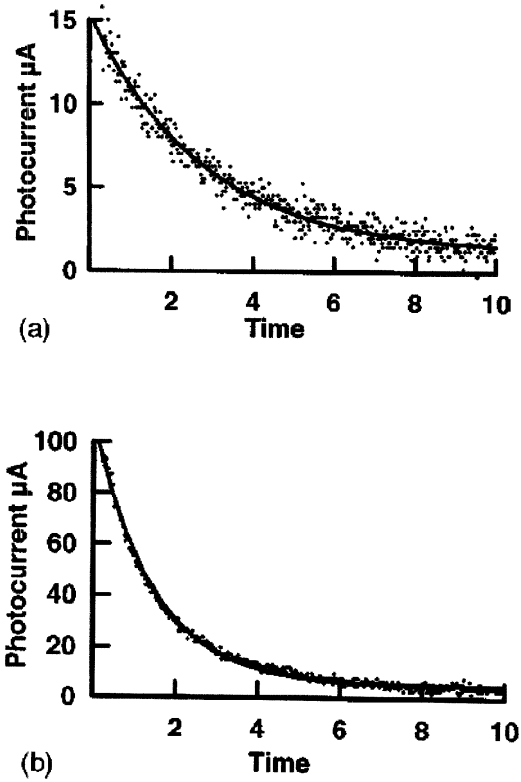

FIGURE 10 Transient photocurrent in crystalline **HAT6** with a) E = 1.5 MV/m. and b) E = 5 MV/m The solid lines show a fit to Eq. (12).

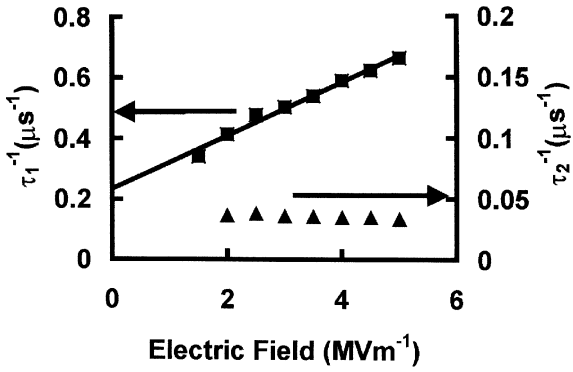

FIGURE 11 The trapping and detrapping rates, τ_1^{-1} and τ_2^{-1} in the crystalline phase of **HAT6** found using the single trap model described in the text.

By fitting these decays it is possible to find the trapping rate, τ^{-1} and the release rate τ_b^{-1}. Figure 11 shows the trapping and release rates found by fitting the decays as a function of the applied electric field. The linear relationship between trapping rate and electric field is indicative of a one dimensional character to the carrier motion. That it does not pass through the origin reflects the fact that the motion is only quasi one dimensional and at low fields carriers will still find traps through diffusion. We speculate that the independence of the release rate with field would be due either to the fact that

a) the trap is a neutral trap which when empty is uncharged and the field has little effect on the binding of the carrier to the trap or
b) that the actual barrier to carrier motion may be an anti-trap in which case again the field would again have little effect.

The possibility that the carriers are halted by barriers or antitraps is interesting as it may explain why, in HAT6 and HAT11, there are transits in the mesophase but not in the crystalline phase. In the mesophase there is a continual exchange of molecules from one stack to the next thus any carrier held up behind a barrier would only have to wait until either the barrier swapped columns or the molecule on which the carrier was swapped columns and its progress continued unhindered. Such a mechanism is unavailable in the crystalline phase where the defects are frozen in.

We note from the transits in these materials that the post transit current tail is very different from material to material. In **2FHAT6** the tail is very short in comparison to the transit time. The same is true of **HAT6** and **HAT11**. By contrast **HAT3** and **HAT6 : PDQ9** have very long post-transit tails compared with the transit time as do **HAT6 : PTP9** and **HAT11 : PTP9**

reported previously. In general the low mobility materials studied here have a short tail compared to the transit time but we must bear in mind that the transit time is long in these materials. If the transit is Gaussian and the post-transit tail is due to diffusion we would expect the ratio of the duration of the tail to transit time to scale as $1/\sqrt{T_{Tr}}$ i.e. the tail would be proportionately smaller as the transit time increased as is found here. However changing the transit time by varying field or sample thickness should also change the relative duration of the tail compared to the transit time. This has been done in Figure 12 where three transits in **HAT11 : PTP9** in the discotic phase are shown normalised to the plateau current and the transit time. The thickness of a sample has been changed from 25.6 μm to 1.5 μm changing the transit time by a factor of 17. They have been displaced vertically for clarity. The curves are identical indicating that the ratio of the tail duration to transit time is not changed and therefore not consistent with a Gaussian transit. The same is true if the transit time is altered through a change in field. There is another large conceptual problem associated with the observed tail in the high mobility materials. If we consider, for instance, the transit shown for **HAT6 : PDQ9** in Figure 5b or that for **HAT3** in Figure 3a, it is clear that the charge under the post-transit tail is greater than that under the pre-transit plateau. This leads us to question the origin of these post-transit carriers i.e. notwithstanding the fact that the inverse transit time is always found to be well

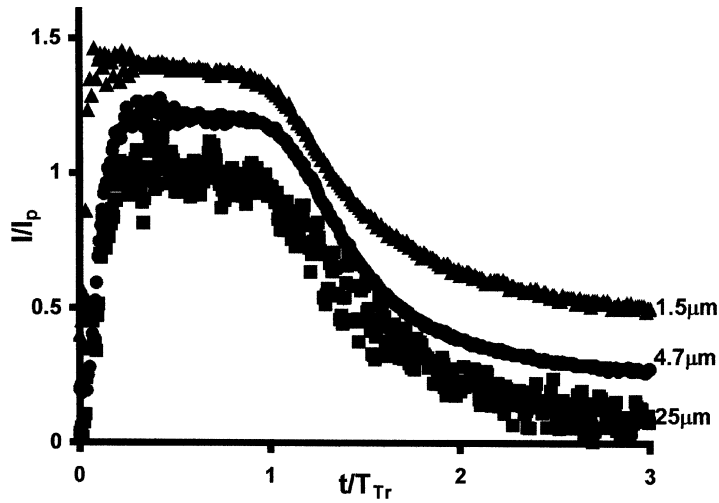

FIGURE 12 Normalised hole photocurrents in discotic (120°C) **HAT11 : PTP9** mixture at various interelectrode spacings of 25.6 μm, 4.7 μm, and 1.5 μm from bottom to top. The three plots are displaced vertically for clarity.

behaved and linear in field for which carriers is it defined? If carriers were falling into deep traps with a dispersion of release rates thus leading to a dispersion in velocity we should expect there to be a fall in the magnitude of the current as time progresses even for the pre-transit current. Yet we have a very flat plateau describing the pre-transit current. Dispersive transits as described in the seminal paper of Montroll and Scher [15], usually show a slowly falling initial current followed by a more rapid fall off after the first transit time. On a log log plot of I verse t such transits deliver a pre and post transit power law with $I(t) \propto t^{1-\alpha}$ followed by $I(t) \propto t^{1+\alpha}$ after the transit. Such dispersive transits do not scale normally with thickness with the mobility increasing with reduced thickness. It is therefore of interest to search for any dependence of the measured mobility on sample thickness in order to rule out dispersive transits. Over a wide range of thicknesses Figure 13 shows the variation in hole mobility of **HAT11 : PTP9** in the middle of the mesophase. To achieve samples with 500 nm electrode spacings required the use of evaporated SiO spacers. Making the sample thin has the undesirable effect of increasing the capacitance and therefore the RC time constant of the measuring circuit whilst at the same time reducing the transit time. For the thinnest sample represented in Figure 13 it was necessary to use an algorithm on the data obtained from a digital oscilloscope to render a transit time observable. On using this algorithm however a transit time could be found and the inverse transit time scaled correctly with field. This work has been reported in full elsewhere [16]. We note here that the variation seen is not inconsistent with the usual variation from sample to sample and that the mobility for the smallest gap has come out of the algorithm and there may therefore be

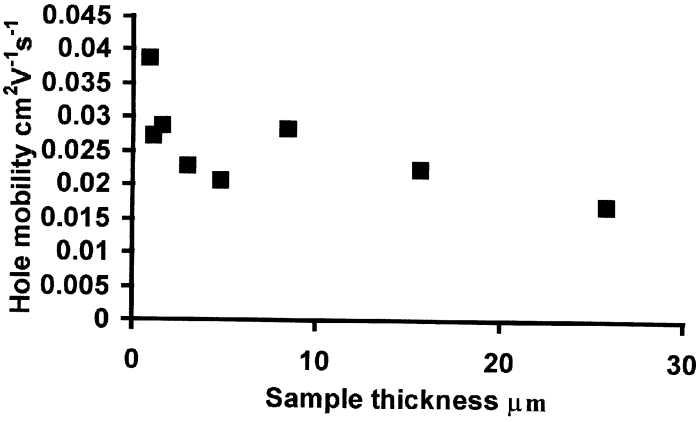

FIGURE 13 The variation of hole mobility in **HAT11 : PTP9** as the sample thickness is varied.

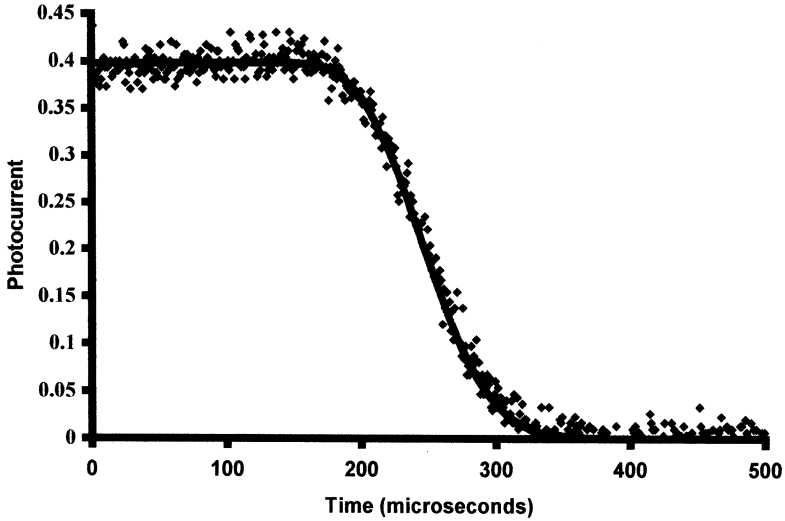

FIGURE 14 A transit photocurrent $I(t)$ for **HAT6** and a fit to the data using the Noolandi multiple trapping model and one set of traps.

some systematic error. There is certainly no strong evidence for anomalous scaling of mobility with field.

An attempt has been made to use the Noolandi model [17] of multiple trapping in a system of traps homogeneously distributed throughout a sample, originally developed to describe anomalous transit-time dispersion in α-Selenium, to describe the transient photocurrents reported here [18]. After Noolandi , the following set of equations describing the free carrier survival fraction, ρ_F and the fraction trapped in a trap of type i, ρ_F are solved.

$$\frac{\partial}{\partial t}\rho(x,t) = g(x,t) - \mu_0 E\frac{\partial}{\partial t}\rho_F(x,t) + D_0\frac{\partial^2}{\partial x^2}\rho_F(x,t) \tag{13a}$$

$$\rho(x,t) = \rho_F(x,t) + \sum_i \rho_i(x,t) \tag{13b}$$

$$\frac{\partial}{\partial t}\rho(x,t) = w_i\rho_F(x,t) - r_i\rho_i(x,t) \tag{13c}$$

The generation rate $g(x,t)$ we choose such as to describe a sheet of charges generated at x = 0 at t = 0 such that

$$g(x,t) = n_f\delta(x)\delta(t)$$

We have kept the diffusion term D_0 unlike Noolandi.

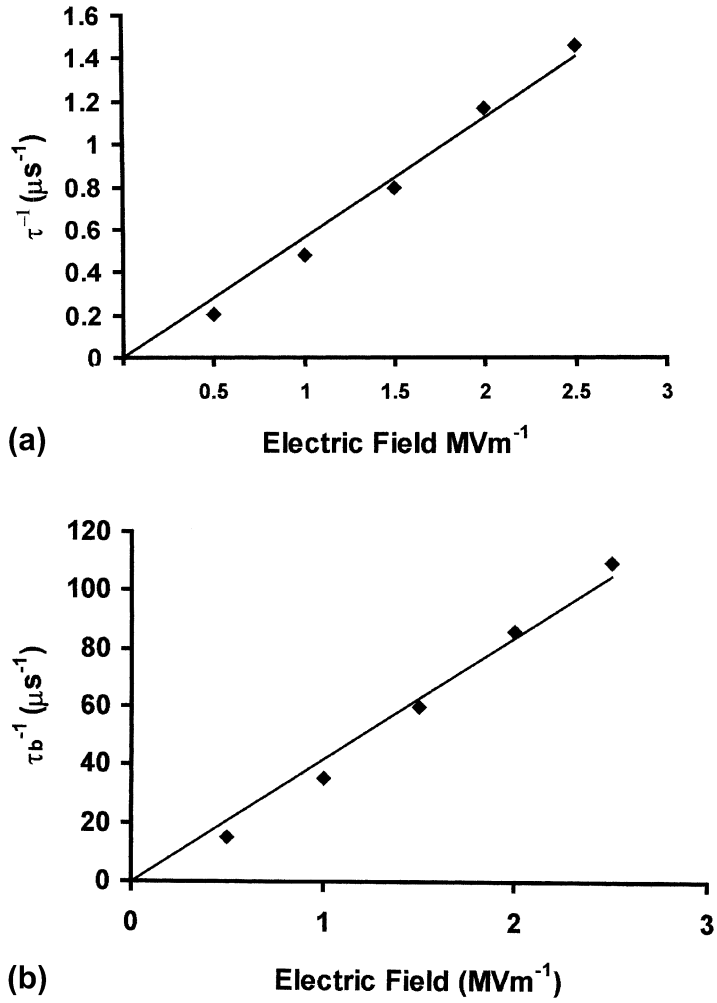

FIGURE 15 a) The variation of trapping rate with electric field found using the Noolandi model to fit transits in **HAT6** in the discotic phase. b) The variation of detrapping rate with electric field found using the Noolandi model to fit transits in **HAT6** in the discotic phase.

The system of equations can be solved by the Laplace--Fourier technique and the current calculated as the mean charge carrier flux between absorbing boundaries with a velocity $\mu_0 E$.

The outcome of these procedures is that the **HAT6** transits can be fitted by a single homogenous trap as shown in Figure 14. Figure 15 shows the

variation of the fitted parameters, trapping rate, τ^{-1} and detrapping rate, τb^{-1}, with electric field. The **HATn : PTP9** mixtures could not be fitted using this model with the homogenous trap distribution. Such distributions cannot deliver a flat plateau along with a long time tail after the transit time. This would appear to be a paradox. One possible resolution yet to be tested is that the transit represents the carriers crossing the sample and reaching the AlO_2 insulator on the counter electrode. As the carriers build up here there will be the evolution of a very large field across the oxide layer until it is sufficient to lower the energy barrier and allow electrons to be injected from the counter electrode in order to recombine with the waiting holes. This hypothesis is currently the subject of an ongoing study.

V. CONCLUSION

In conclusion, TOF mobility measurements have been presented for 5 new materials including 3 binary systems. They have been compared with four materials previously reported. The binaries consistently show a higher mobility until the **HATn** aliphatic chain falls below $n = 5$. The binaries and $n < 5$ triphenylenes also display an increased range and transit in the crystalline phase. The temperature dependence of the mobility has been carefully studied for each of these systems and while it is often very slowly varying with temperature there are exceptions. A model of the small polaron is able to describe all the μ versus T results with reasonable values of the parameters, the polaron energy and bandwidth, emerging from the analysis.

The one dimensionality of the systems is shown up when there is trapping by using a simple single trap model in the case of **HAT6** in the crystalline phase and a more sophisticated model of multiple trapping due to Noolandi in the mesophase of **HAT6** where we have transits. In the Noolandi case there is still the need for only one type of trap to reproduce the experimental results. For both models a trapping rate proportional to electric field is obtained. In the transit regime using the Noolandi model the detrapping rate is also inversely proportional to electric field.

We have no adequate explanation for the anomalous scaling of the transient photocurrents in the case of the binary mixtures and **HAT3** and **2FHAT6**. Dispersive transport does not offer an explanation for these observations although there may exist an answer due to charge build up at an oxide interface. The resolution of this paradox awaits further work.

REFERENCES

[1] Boden, N., Bushby, R. J., Clements, J., Movaghar, B., Donovan, K. J., & Kreouzis, T. (1995). *Phys. Rev. B.*, *32*(18), 13,274.

[2] Kreouzis, T., Scott, K., Donovan, K. J., Boden, N., Bushby, R. J., Lozman, O. R., & Liu, Q. (2000). *Chem. Phys.*, *262*, 489.
[3] Donovan, K. J., Kreouzis, T., Boden, N., & Clements, J. (1998). *J. Chem. Phys.*, *109*(23), 10,400.
[4] Nakayama, H., Ozaki, M., Schmidt, W. F., & Yoshino, K. (1999). *Jpn. J. Appl. Phys.*, *38*, L1038.
[5] Kreouzis, T., Donovan, K. J., Boden, N., Bushby, R. J., & Lozman, O. R. (2001). *J. Chem. Phys.*, *114*, 4, 1797.
[6] Boden, N., Bushby, R. J., Lozman, O. R., & Wood, A. (2000). *Angew. Chem.*, *39*(13), 2333.
[7] Adam, D., Schuhmacher, P., Simmerer, J., Haussling, L., Siemensmeyer, K., Etzbach, K. H., Ringsdorf, H., & Haarer, D. (1994). *Nature*, *371*, 141.
[8] Adam, D., Closs, F., Frey, T., Funhoff, D., Haarer, D., Ringsdorf, H., Schuhmacher, P., & Siemensmeyer, K. (1993). *Phys. Rev. Lett.*, *70*, 457.
[9] Palenberg, M. A., Silbey, R. J., Malagoli, M., & Bredas, J.-L. (2000). *J. Chem. Phys.*, *112*, 3, 1541.
[10] Holstein, T. (1959). *Annals of Physics*, *8*, 325.
[11] Holstein, T. (1959). *Annals of Physics*, *8*, 343.
[12] Pope, M. & Swenberg, C. E. (1982). "*Electronic Processes in Organic Crystals*", Clarendon Press: Oxford.
[13] Montroll, E. W. & Weiss, G. H. (1965). *J. Math. Phys.*, *6*, 167.
[14] Haarer, D. & Mohwald, H. (1975). *Phys. Rev. Letts.*, *34*, 23, 1447.
[15] Scher, H. & Montroll, E. W. (1975). *Phys. Rev. B.*, *12*, 6, 2455.
[16] Donovan, K. J. & Kreouzis, T. (2000). *J. App. Phys.*, *88*, 2, 918.
[17] Noolandi, J. (1977). *Phys. Rev. B.*, *16*(10), 4466.
[18] Pecchia, A., Lozman, O. R., Movaghar, B., Boden, N., Bushby, R. J., Donovan, K. J., & Kreouzis, T. (2002). *Phys. Rev. B.*, *65*, 104204.